Computers and Concrete, *Vol. 23, No. 1 (2019) 69-80*
DOI: https://doi.org/10.12989/cac.2019.23.1.069

Numerical study of ITZ contribution on diffusion of chloride and induced rebar corrosion: A discussion of three-dimensional multiscale approach

Xi Tu[*1,2], Cunjun Pang[1,2], Xuhong Zhou[1,2] and Airong Chen[3]

[1]*Key Laboratory of New Technology for Construction of Cities in Mountain Area (Chongqing University), Ministry of Education, Chongqing, China*
[2]*College of Civil Engineering, Chongqing University, Chongqing, China*
[3]*Department of Bridge Engineering, Tongji University, Shanghai, China*

(Received August 24, 2018, Revised January 23, 2019, Accepted January 30, 2019)

Abstract. Modeling approach for mesoscopic model of concrete depicting mass transportation and physicochemical reaction is important since there is growing demand for accuracy and computational efficiency of numerical simulation. Mesoscopic numerical simulation considering binder, aggregate and Interfacial Transition Zone (ITZ) generally produces huge number of DOFs, which is inapplicable for full structure. In this paper, a three-dimensional multiscale approach describing three-phase structure of concrete was discussed numerically. An effective approach generating random aggregate in polygon based on checking centroid distance was introduced. Moreover, ITZ elements were built by parallel expanding the surface of aggregates on inner side. By combining mesoscopic model including full-graded aggregate and macroscopic model, cases related to diffusivity and thickness of ITZ, volume fraction and grade of aggregate were studied regarding the consideration of multiscale compensation. Results clearly showed that larger analysis model in multiscale model expanded the diffusion space of chloride ion and decreased chloride content in front of rebar. Finally, this paper addressed some worth-noting conclusions about the chloride distribution and rebar corrosion regarding the configuration of, rebar diameter, concrete cover and exposure period.

Keywords: reinforced concrete structure; chloride diffusion; numerical simulation; multiscale; ITZ

1. Introduction

Corrosion of rebar induced by chloride ion could significantly deteriorate the serviceability of concrete structures (Zhu *et al*. 2016). The protective film of rebar was depassivated by chloride ion penetrated from surface of concrete and thus corrosion of rebar initiates once the chloride content on surface of rebar reach a certain thresholding value, defined as critical chloride content. Afterwards, corrosion of rebar keeps propagating and induces further cracking and spalling due to expansion of rust. Therefore, it is important to accurately assess the diffusion process of chloride ion within concrete, which is meaningful for further evaluation of durability of reinforced concrete structures.

In the view of mesoscopic numerical simulation, concrete was recognized as the heterogeneous composite of three phases, including cement paste, aggregate and Interfacial Transition Zone (ITZ). ITZ was identified as a fine cement paste zone enclosing aggregate and rebar, providing higher water-to-cement ratio, higher porosity and lower cement content compared with normal bulk cement paste regions. Thus ITZ was generally considered as an individual phase (Angst *et al*. 2009, Zheng *et al*. 2009). Though the porosity of ITZ decreases with increase of distance from aggregate surface (Xu and Li 2017), ITZ was simplified as a homogenous thin layer in most study. Significant influence on the overall behavior of concrete attributes to ITZ due to its fraction of the total paste volume, such as diffusivity and strength (Bernard and Kamali-Bernard 2015, Du *et al*. 2014, Xu and Li 2017, Zheng *et al*. 2009).

In the view of mesoscopic numerical simulation, due to large amount of nodes and elements, an optimized approach was that three-phase composite of concrete was simplified into two-phase composite including cement paste and homogenized equivalent aggregate (Du *et al*. 2014, Wu *et al*. 2015, Zhang and Zhang 2017, Zhang and Zhang 2018, Zheng *et al*. 2009, Zheng and Zhou 2013). Diffusivity of ITZ was transferred by means of deriving the analytical solution of general effective chloride diffusivity, which means modeling of ITZ is unnecessary.

Generally, modeling and analysis for cement-based material were categorized in microscopic scale, mesoscopic scale and macroscopic scale. (Unger and Eckardt 2011). Recently a number of theory research and modeling efforts have been devoted to studying multiscale modeling. Multiscale modeling was usually defined as the integrated numerical process of transferring mechanical and chemical response between lower scale and higher scale (Chen *et al*. 2016, Maekawa *et al*. 2003). A significant advantage of multiscale modeling is optimizing computing loading and enhancing the precision. According to available literature, researchers generally focused on the transferring process of material response between scales.

As the major purpose of multiscale modeling to reduce

∗Corresponding author, Ph.D.
E-mail: tuxi@cqu.edu.cn

ISSN: 1598-8198 (Print), 1598-818X (Online)

calculation loading, heterogeneous model was always modeled for transferring damage and mass transportation of critical regions from the macroscale to the mesoscale which provided coupling of sub-domains (Hiratsuka and Maekawa 2015). Balance of accuracy and efficiency is the major consideration of multiscale modeling for numerical simulation. By means of macroscopic model substituting for a part of mesoscopic model, multiscale modeling is able to provide relatively smaller size of mesoscopic model, generate the same filling rate of aggregate and less amount of aggregate, which is no doubt beneficial for raising success rate of meshing (Tu *et al*. 2018).

For mesoscopic structure of concrete, both of size and shape of aggregates are generated as given design. Regarding two-dimensional space, general process was divided into two steps, including modeling of geometric model and meshing. Angular aggregate was generated based on inscribed convex polygon within elongated ellipse (Wang *et al*. 2016). Wang proposed a procedure for generating random aggregate structures for angular aggregates by means of Monte Carlo sampling, which was compatible for concave polygon (Wang *et al*. 1999). An inevitable algorithm was intersection check of convex polygons, which was achieved by detecting space independence of two polygons (Bailakanavar *et al*. 2012, Ren 2006). In terms of meshing, mortar plus smaller aggregates embedding coarse aggregate was discretized into finite elements by free meshing (Caballero *et al*. 2006, Wang *et al*. 2016) or uniform Background grid (Biondini *et al*. 2004, Ma *et al*. 2016, Šavija *et al*. 2013a).

Another major factor for durability of reinforced concrete structures is corrosion of steel rebar. Researchers devoted efforts on laboratorial research by means of natural experiments (François and Arliguie 1999, Vidal *et al*. 2004, Vidal *et al*. 2007, Zhang *et al*. 2009, Zhang *et al*. 2010) and accelerated experiments (Andrade *et al*. 1993, Li 2000, Liu and Weyers 1998, Pritpal and Mahmoud 1999, Torres-Acosta *et al*. 2007, Torres-Acosta Andrés and Martı´nez-Madrid 2003) about the process of chloride diffusion and corrosion. On the other hand, some types of simplified approximate law for corrosion were introduced. Biondini introduced a reasonable linear damage model for corrosion of rebar under aggressive agent, which evaluates corrosion rate according to the real-time chloride content surrounding rebar (Biondini *et al*. 2006). Despite of the complex principle of corrosion, based on the natural damage mode of corrosion, this linear damage model is able to provide acceptable description of damage process.

This paper discussed two important aspects regarding multiscale modeling for numerical simulation of chloride ion diffusing within concrete. Firstly, a comprehensive modeling approach for concrete considering both multiscale modeling including Interfacial Transition Layer (ITL) and three-phase mesoscale structure including ITZ. Secondly, by means of the multiscale numerical simulation tool, the influence of ITZ on diffusion of chloride ion within concrete in mesoscale was studied in detail, where ITZ was modeled as an individual phase in FE model for chloride diffusion in concrete. Besides, the corrosion of rebar in straight edge of concrete induced by diffusion of chloride ion was also calculated to study the time evolution of corrosion process.

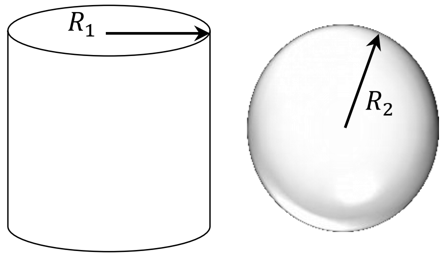

(a) Sphere vs. cylinder

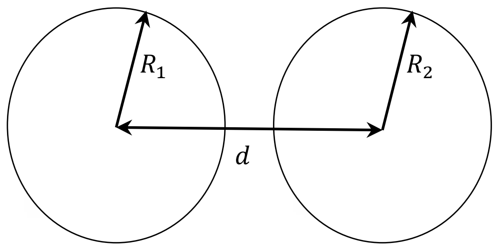

(b) Distance of sphere and cylinder in axial view

Fig. 1 Determining overlapping of sphere and cylinder

2. Mesoscopic multiscale modeling approach

2.1 Generation of random spherical aggregate model in three-dimensional space

The major consideration of generating mesoscopic model is the requirement of both grading of aggregates and its volume fraction in concrete. Generally, the mesoscopic structure of aggregate is randomly generated by dispersing particles in given shape and size in a limited square or rectangle space. This process was fulfilled by two essential steps, including constructing qualified aggregate and dispersing the aggregate. Generally, actual shape of aggregate in three-dimensional space was recognized as polyhedron. However, considering the complexity and efficiency of generating random polyhedron and corresponding determination of overlapping, sphere was an optimized shape for further study due to the convenience of modeling.

1) Construction of spherical aggregate in given size regarding grading of concrete

Regarding the filling rate of aggregate, the diameter (particle size) and volume of each spherical aggregate was calculated according to the grading of concrete.

2) Dispersing aggregate by judgement of overlapping of aggregate and steel rebar

In three-dimensional space, steel bar within concrete was always represented by cylinder. The relationship of sphere and cylinder in three-dimensional space was demonstrated in Fig. 1. Whether overlapping of both volumes appeared was controlled by the distance from centroid of sphere to axis of cylinder. Assuming radius of cylinder and sphere were R_1 and R_2 respectively. the distance from the centroid of sphere to the axis of cylinder was d. Thus for the case of $d \geqslant R_1+R_2$, no overlapping for existing rebar and aggregate occur and vice versa.

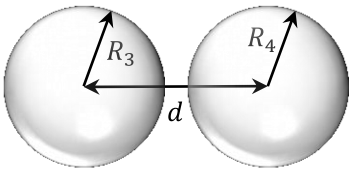

Fig. 2 Distance between two spherical aggregates

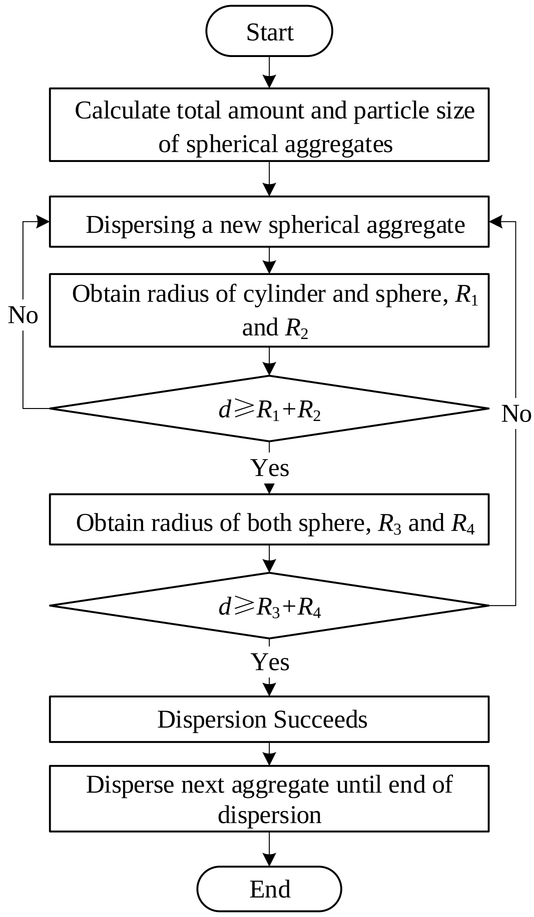

Fig. 3 Process of generating random spherical aggregates

3) Dispersing aggregate by judgement of overlapping of aggregates

Similar judgement for two spherical aggregates was considered compared with the case between spherical aggregate and cylindrical steel bar, shown in Fig. 2. Thus for the case of $d \geqslant R_3+R_4$, no overlapping for existing rebar and aggregate occurs and vice versa.

The above proposed approach was illustrated in the process in Fig. 3. An obtained sample aggregate model was shown in Fig. 4.

Additional process for modeling is meshing the geometry space including significantly irregular distribution of aggregate. Conventional commercial software was adopted for meshing process. However, low success rate of meshing in refined hexahedral elements cannot be avoided for most commercial software due to the complex model. Thus an optimized way adopted in this paper was meshing the space in tetrahedron element, which was proved as high meshing success rate and high efficiency.

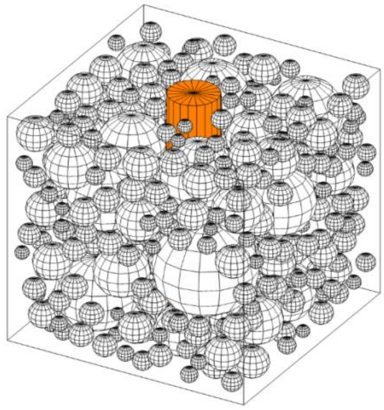

Fig. 4 A generated aggregate model (White) within existing cylindrical steel bar (Orange)

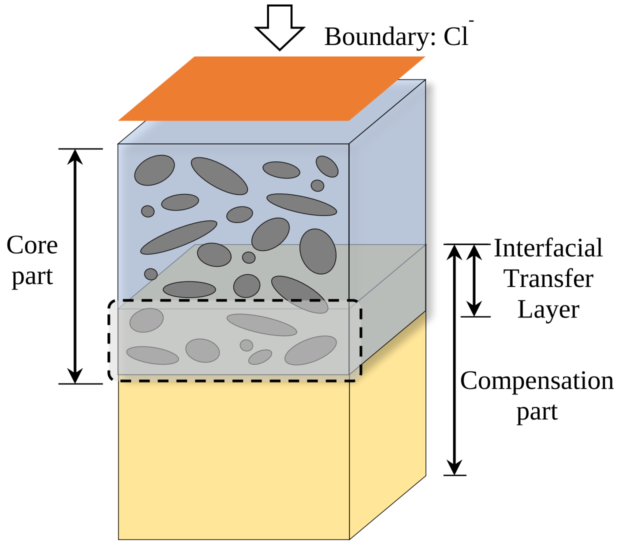

Fig. 5 3D multiscale model with Core part and Compensation part for simulating chloride diffusion within concrete

2.2 Multiscale approach for compensation

Complexity of FE model is the major difficulty for mesoscopic simulation of chloride diffusion, especially for the model including individual elements of ITZ. Generally, 200mm or less was recognized as the optimized edge length for square or rectangle of analysis space due to maximum particle size of aggregate, limitation of computing resource and acceptable accuracy in mesoscale. Moreover, for a typical period of exposure, penetration of chloride ion throughout the whole analysis space was inevitable and thus a larger space is needed in case of additional deviation. Moreover, with maintaining the same grading curve of course aggregate, topological complexity of geometric structure largely weakens the success rate of meshing and becomes another obstacle for numerical simulation.

Multiscale modeling was proved as a reasonable solution regarding the above limitations and meanwhile balances amount of nodes and elements and calculation accuracy (Tu *et al*. 2018). In the light of this approach, in three-dimensional space, original mesoscopic model (Core

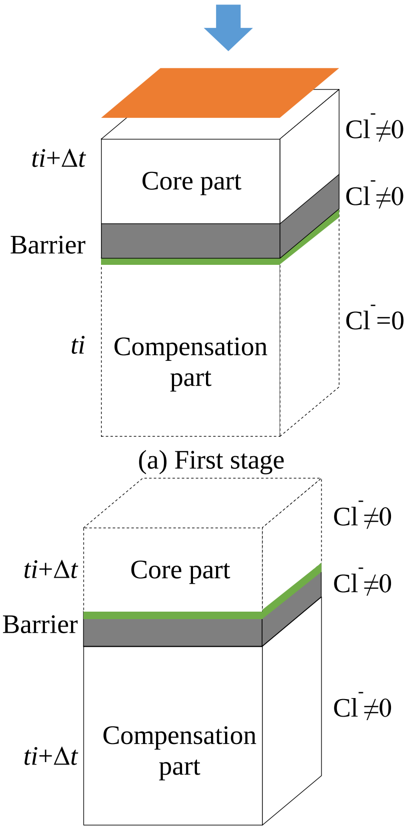

(a) First stage

(b) Second stage

Fig. 6 The two stages of chloride diffusion at interfacial transition layer connecting macroscopic and mesoscopic model

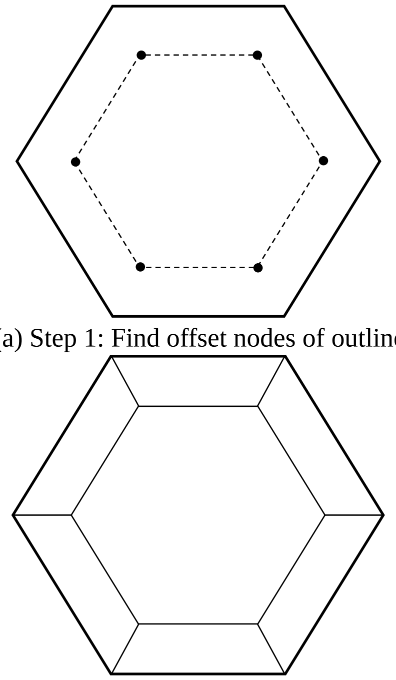
(a) Step 1: Find offset nodes of outline

(b) Step 2: Form elements of ITZ

Fig. 7 Process of generating new elements and nodes for ITZ in the view of cross section of 3D meshed outline of aggregate

part) including cement paste, aggregate and ITZ was coupled with a newly introduced and simplified macroscopic model (Compensation part), which formed a new and larger space for chloride diffusion compared with previous way (Fig. 5).

Due to different definition of nodal chloride content and diffusion coefficient in both model, the overlapped zone in both parts was defined as Interfacial Transition Layer (ITL), shown in Fig. 5. ITL was designed as a banded shape transition zone composing by a group of nodes and elements and provided the redistribution channel for core part and compensation part. Equivalent diffusivity and distribution of chloride content in both model were calculated within the range of ITL.

The process of transferring chloride ion within ITL was illustrated in Fig. 6. For initial state, Analysis space of three phases including core part, compensation part and ITL was modeled respectively. Boundary condition was set at surface of concrete, which was the top of core part shown in Fig. 6.

This mixed model behaved in sequential multiscale process. For the mixed case that core part is in mesoscale and compensation part in macroscale, equivalent chloride content in ITL will be calculated and transferred. Definitions of chloride content in both parts were different. Chloride content in macroscopic model was measured in concrete and the value in mesoscopic model was measured in cement. Therefore, a necessary procedure was included that the value of chloride content in ITL should be calculated for each stage. Simulation of chloride diffusion within mixed model was divided into two stages of diffusion and two steps of conversion.

1) The first stage of diffusion

Core part and ITL were connected as common interface while ITL and compensation part were disconnected. With one time-step, chloride ion penetrated into core part from boundary condition. During current stage, diffusion of chloride ion restrained within core part and ITL. The chloride content of core part and ITL rose up from previous content while compensation part kept unchanged. Find out all of the elements with the centroid located within the elements from compensation model. Calculate the weighted mean content of all these elements in core model. This content is the represented content for the element in compensation model.

2) Conversion from mesoscale to macroscale within ITL

The simulated result in region in core part covered by ITL was converted from mesoscale to macroscale within this step. For the instance of center bottom of concrete boundary, compensation part was modeled as simply macroscopic model which is equivalent as the averaged mesoscopic model. Within core part, elements with their centroid included in Interfacial Transfer Layer were identified. Weighted mean value of chloride content of these involved elements was calculated for the nodal value of ITL in macroscale.

3) The second stage of diffusion

A new barrier was inserted at common border of core part

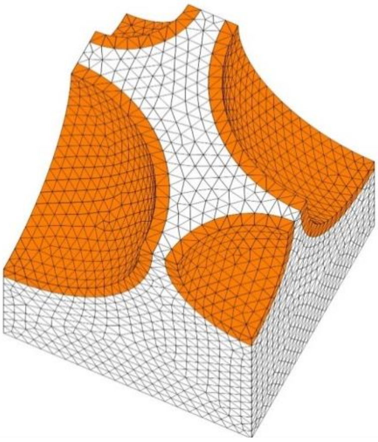

Fig. 8 Smaple of generated ITZ elements (Orange) adhering original meshed aggregate model (White)

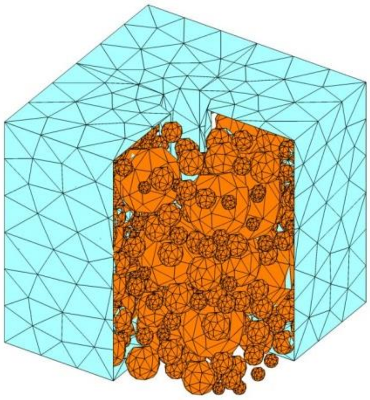

Fig. 9 Smaple of generated ITZ elements (Orange) and original aggregate model (Blue)

and ITL which was equal to cut down the connection of these parts. The existing barrier at common border of compensation part and ITL was removed. During this stage, chloride redistributes within the region including ITL and compensation part.

4) Conversion from macroscale to mesoscale within ITL

As the inverse process of the 2nd step, the nodal content of mesoscopic core part was interpolated from macroscopic compensation part in the form of regular rectangle element. As was illustrated in Fig. 4, the outer rectangle represents the uniform quadrilateral model in compensation part and the target node denotes the node included within core part. Four nodes of the quadrilateral were numbered in counterclockwise.

2.3 Modeling of ITZ based on meshed space

Modeling approach for ITZ was determined by the mechanism of simulating chloride diffusion within ITZ. ITZ was recognized as an indeterminate zone around aggregates and bulk, in linearly decreasing porosity with increase of distance from aggregate surface. Existing approaches describe ITZ as an individual layer or compensation on equivalent diffusivity of aggregate (Dridi 2013, Sun *et al*. 2011, Zhu *et al*. 2017). In terms of aggregates in random

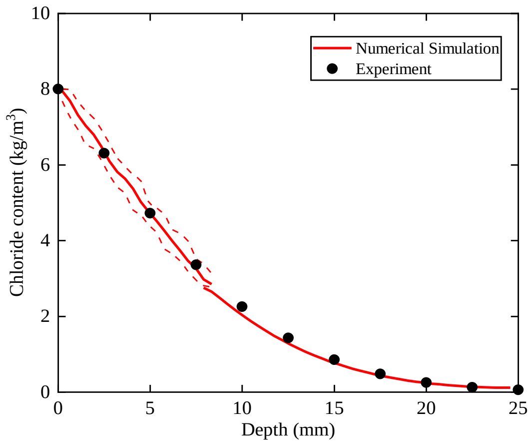

Fig. 10 Comparison of profiles and envelop of chloride content regarding compensation for numerical simulation and experimental measurement by Mori *et al*. (2006)

polygon, the way of building actual elements of ITZ was adopted in this paper. Thus more DOFs were introduced, which significantly increased time consumption of assembling global diffusion matrix and solving it.

Since ITZ was identified as the individual phase surround aggregate, additional uniform thickness of elements adhering on the surface of aggregates might induced unnecessary overlapping of ITZ elements in some cases that the pair of aggregate were too close to each other. In order to avoid the above circumstance, ITZ elements were assigned on the inner side of surface of aggregate instead of outer side. According to minor area proportion of ITZ, it was acceptable slightly decreasing the size of aggregate. There are totally two steps for this process.

• For the first step, all nodes of the offset surface were found, the total number of which were equal to vertices of aggregate, shown as the black point in Fig. 7(a).

• For the second step, combining the previous available nodes of aggregate and newly generated nodes (intersection), a group of tetrahedron elements were built, which represented ITZ. Their physical properties were set individually being different from existing cement paste.

2.4 Verification

Though the effect of ITZ on chloride diffusion is still arguable, numerical simulation easily shows the significant impact of ITZ on its results. The comparative study with experimental results is considered. 2D distribution of chloride ingress observed by Mori *et al*. (2006) was used to verify the proposed model in this paper. As listed in the literature, 46% equivalent filling percentage of aggregate for mesoscopic model was considered. The condition of exposure was 3% NaCl solution at 20℃ for 91 days. Thus boundary condition and diffusion coefficient were set as 8 kg/m^3 and 5.50×10^{-12} m^2/s respectively. Equivalent diffusion coefficient for mesoscopic model was calculated regarding the distribution of effective aggregate gradation of mesoscopic model. Binding of chloride ion was neglected.

Fig. 10 indicated the comparison of results from the specimen investigated exposed in designed experimental environment by numerical simulation and experimental measurement. According to the obtained diagram, the result from numerical simulation agreed well with experimental measurement, which can conclude the numerical approach is practical.

3. Statistical assessment of chloride diffusion

3.1 Influence of ITZ properties regarding compensation

Considering that characteristics of ITZ significantly influence diffusion chloride within concrete, critical properties of ITZ were detailed studied in this section, including diffusivity and thickness of ITZ, aggregate volume fraction and grade of aggregate. Furthermore, chloride content on surface of rebar was also researched regarding presence of ITZ.

Another major consideration of this paper was the effect of compensation in multiscale modeling. A 100×100×100 mm three-dimensional cubic space was modeled for mesoscopic core part and another 100×100×200 mm cubic space was modeled for macroscopic compensation part. Thickness of ITL was set at 10 mm, which means 10% area of core part and 5% area of compensation part were overlapped. On the other hand, for the case without compensation, macroscopic compensation part was deleted and chloride ion can only diffuse within smaller space of mesoscopic core part.

For the other parameters, transportation mechanism of chloride ion between both parts was described in previous section of this paper. For all simplified cases studied in this section, the analytical apparent surface chloride content of 0.708 (% w_c) and apparent concrete diffusivity of 1.837×10^{-12} m^2/s were adopted for macroscopic model, which were regressed based on the Zhao's data (Zhao *et al*. 2009). An equivalent diffusivity of cement considered for mesoscopic core model was calculated in terms of volume fraction of concrete. Meanwhile, aggregate was considered as impermeable and corresponding modeling of FEM was ignored. Boundary condition and diffusivity of cement paste were calculated by these result. Regarding generating random aggregate of mesoscopic model, Fuller's curve was adopted as the grading of aggregate. Both types of cases with compensation and without compensation were studied.

Significant random distribution of aggregate was the major factor for uncertainty of chloride diffusion. Thus totally 100 specimens of aggregate model for each case were generated and analyzed considering reasonable accurate and acceptable time consumption. After all specimen were analyzed, mean results of these cases were calculated for further comparison.

3.1.1 Diffusivity of ITZ

Firstly, diffusivity of ITZ was studied, which was represented by the ratio of D_{ITZ}/D_{CP}. Here, D_{ITZ} and D_{CP} denoted the diffusivity in ITZ and cement paste respectively. As was discussed by Zheng (Zheng *et al*. 2009), D_{ITZ}/D_{CP} would vary within 1~5 considering different configuration of w/c, aggregate size, hydration time and aggregate fraction

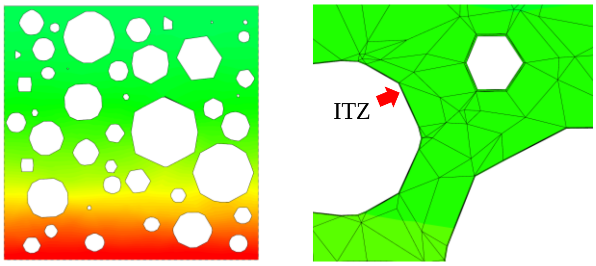

(a) Sliced section of concrete (b) Detail of meshed model within ITZ

Fig. 11 Typical distribution of chloride content regarding diffusivity in ITZ

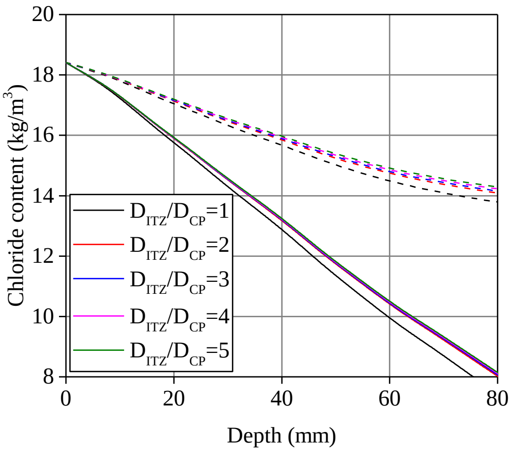

Fig. 12 Average content vs. depth, regarding compensation and ITZ D_{ITZ}/D_{CP}, 50yr of exposure (Dashed: w/o compensation; Solid: with compensation)

theoretically, which were discussed by means of the approach introduced in this paper. 50µm of ITZ thickness was modeled by expanding the edge of aggregate and rebar. Maximum aggregate size in 20mm was considered.

Fig. 11 showed typical distribution of chloride content regarding different diffusivity in ITZ. The major difference of contour line was observed slightly higher chloride content due to the presence of ITZ in thickness of micrometer scale. It means higher diffusivity in ITZ compared with cement paste accelerated the diffusion of chloride within concrete.

For mesoscopic numerical simulation, distribution of aggregate was recognized as the major influence factor for development of chloride (Pan *et al*. 2015). Chloride content on surface of rebar significantly varied with different arrangement and grading of aggregate. Thus both mean and maximum distribution of chloride ion in terms of random aggregate models became the major consideration. Fig. 12 and Fig. 13 summarized average content & maximum versus depth regarding diffusivity of ITZ at 50 years and 100 years respectively. It was clearly noted that chloride content increased as the diffusivity of ITZ increased. An interesting phenomenon observed was that the influence of compensation was larger in higher chloride content. It attributed to a larger diffusion space released in mixed model including compensation part. From the result of numerical simulation, another point should be noted that within the boundary layer in thickness of 10 mm from surface of

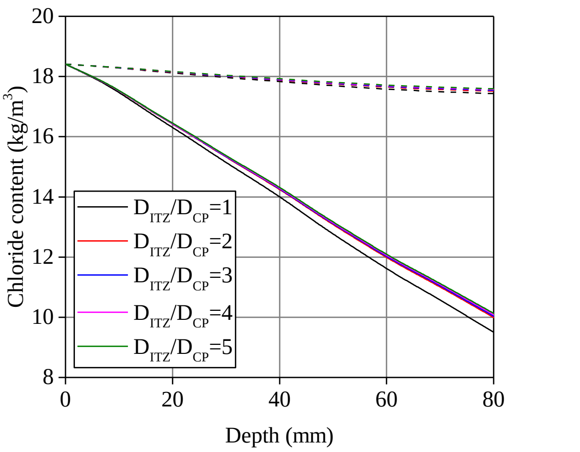

Fig. 13 Average content vs. depth, regarding compensation and ITZ D_{ITZ}/D_{CP}, 100yr of exposure (Dashed: w/o compensation; Solid: with compensation)

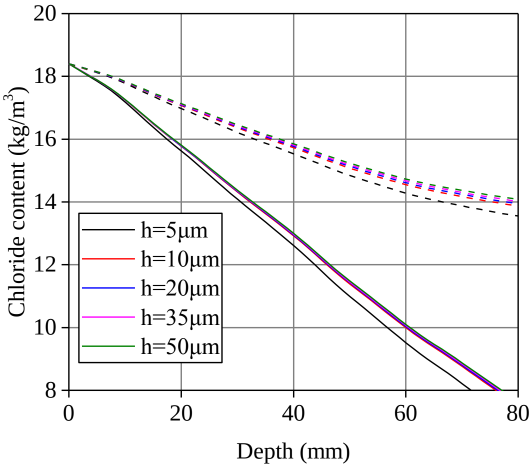

Fig. 14 Average content vs. depth, regarding compensation and ITZ thickness, 50yr of exposure (Dashed: w/o compensation; Solid: with compensation)

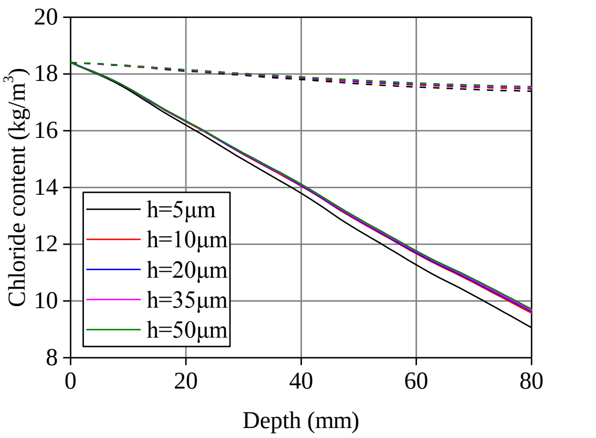

Fig. 15 Average content vs. depth, regarding compensation and ITZ thickness, 100yr of exposure (Dashed: w/o compensation; Solid: with compensation)

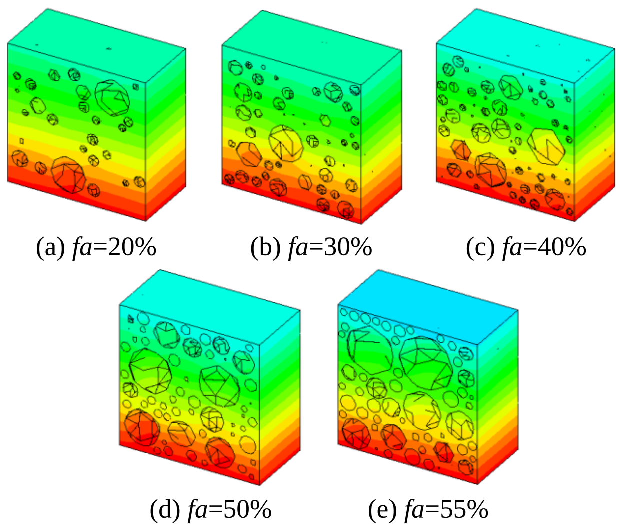

Fig. 16 FE model and typical distribution of chloride content for different aggregate volume fraction, *fa*

concrete, both mean and maximum chloride content were closed to boundary condition, which was recognized as the lower aggregate volume fraction and smaller particle size in this region.

3.1.2 ITZ thickness

The second major factor for chloride diffusion is ITZ thickness. A thin layer composing by quadrilateral elements in the thickness of 5 μm, 10 μm, 20 μm, 35 μm and 50 μm adhering to the edge of aggregates was modeled. For the other parameters, diffusivity of ITZ in D_{ITZ}/D_{CP}=5 was adopted. Maximum particle size of coarse aggregate was limited within D_{max}=20 mm.

Fig. 15 showed average content and maximum versus depth regarding thickness of ITZ at 50 years and 100 years respectively. A clear conclusion was drawn that larger ITZ thickness induced higher volume fraction of ITZ and enhanced diffusion of chloride ion.

3.1.3 Aggregate volume fraction

Aggregate volume fraction determined total amount of aggregates within given space and accordingly total length of perimeter was also determined, which was the key factor for proportion of ITZ in concrete. In this section, the cases of aggregate volume fraction in 20%, 30%, 40%, 50%, 55% were discussed by means of the approach introduced in this paper. Diffusivity of ITZ in D_{ITZ}/D_{CP}=5 and 50 μm of ITZ thickness were adopted. Maximum aggregate size in 20 mm and Fuller grading was adopted. Both types of cases with compensation and without compensation were studied. Fig. 16 showed with aggregate volume fraction from 20% to 55%, the typical distribution of chloride content and aggregate with given analysis square space.

Fig. 17 described mean content & maximum versus depth regarding aggregate volume fraction at 50 years. According to the result, presence of ITZ provided greater effect on higher aggregate volume fraction and thus reduced the difference of chloride content profile in cases with different aggregate volume fraction.

3.1.4 Grade of aggregate

The cases for grade of aggregate with maximum

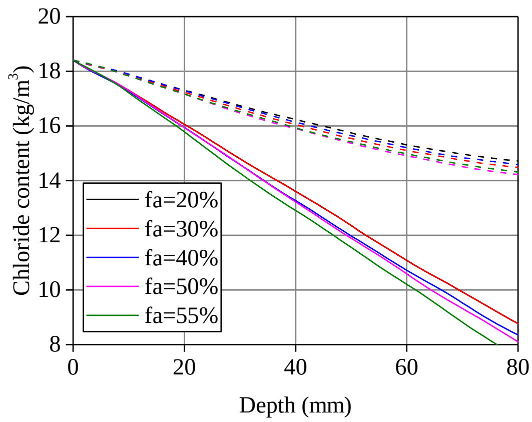

(a) Mean chloride content with ITZ

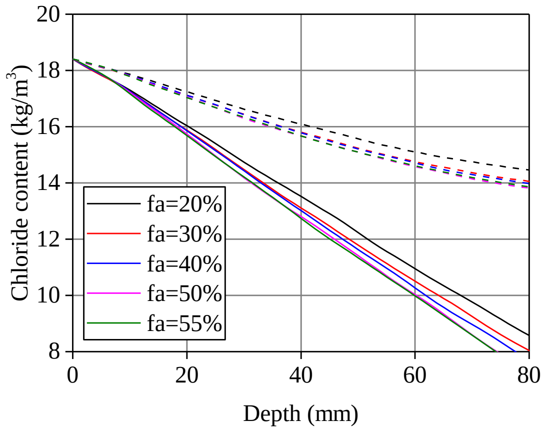

(b) Mean chloride content w/o ITZ

Fig. 17 Average content vs. depth, regarding aggregate volume fraction (fa) and presence of ITZ, 50yr of exposure (Dashed: w/o compensation; Solid: with compensation)

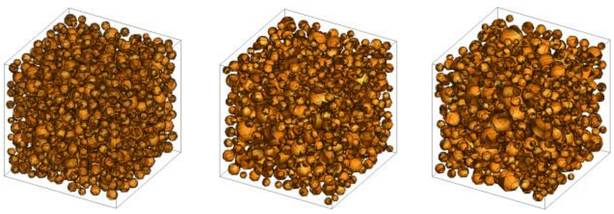

(a) D_{max}=15 mm (b) D_{max}=20 mm (c) D_{max}=25 mm

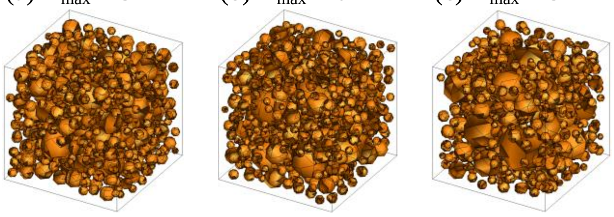

(d) D_{max}=30 mm (e) D_{max}=35 mm (f) D_{max}=40 mm

Fig. 18 FE model and typical distribution of chloride content for different aggregate and gradation

aggregate size D_{max}=5 mm, 10 mm, 15 mm, 20 mm, 25 mm, 30 mm were discussed. Both cases with or without ITZ were included. Fuller grading was adopted. For the case with ITZ, Diffusivity of ITZ in D_{ITZ}/D_{CP}=5 was adopted. 50 μm of ITZ thickness was modeled by expanding the edge of aggregate and rebar. Both types of cases with compensation and

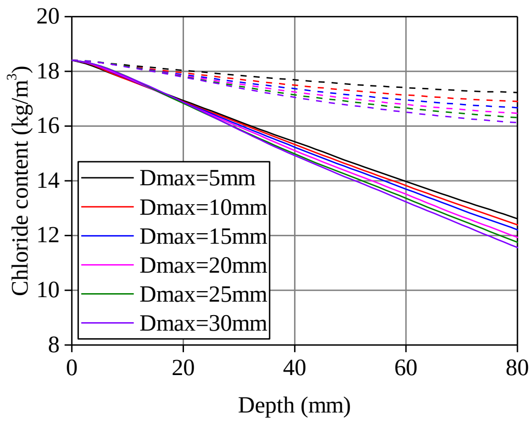

(a) Mean with ITZ

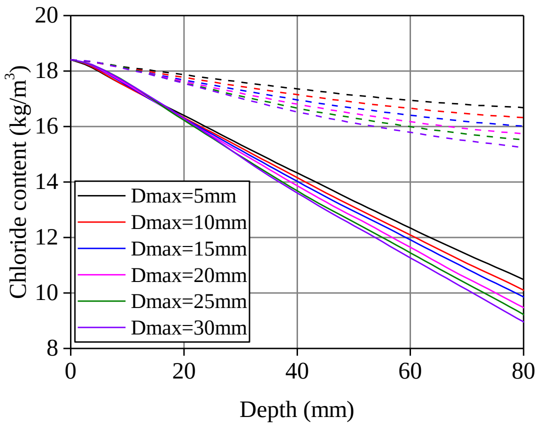

(b) Mean w/o ITZ

Fig. 19 Average content vs. depth, regarding grade of aggregate and presence of ITZ (Dashed: w/o compensation; Solid: with compensation)

without compensation were studied. Fig. 18 showed with maximum aggregate size from 5 mm to 30mm, the typical distribution of chloride content and aggregate with given analysis square space. Fig. 19 showed mean content & maximum versus depth regarding grade of aggregate at 50 years.

Fig. 19 summarized mean and maximum chloride content vs. depth from surface of concrete. An interesting point should be noted that the lower aggregate volume fraction and smaller particle size in the region closed to boundary was not significant in the case with smaller maximum particle size. Moreover, presence of ITZ indeed enhanced diffusion of chloride ion especially in cases with smaller maximum particle size.

3.2 Chloride content and corrosion of steel rebar

In this section, chloride content on the front of rebar in terms of the configuration was studied by the multiscale numerical simulation introduced previously. According to general engineering design, a group of concrete cover thickness and rebar diameter were devised for detailed comparison of chloride diffusion and rebar corrosion, shown in Table 1. For the purpose of comparison, rebar in diameter of 16 mm was selected for the cases in different cover

Table 1 Details of model comparison for concrete cover thickness and rebar diameter regarding chloride diffusion and rebar corrosion

Cover thickness, C (mm)	Rebar diameter, D (mm)				
	12	16	20	25	28
20		×			
30		×			
40		×			
50	×	×	×	×	×
60		×			

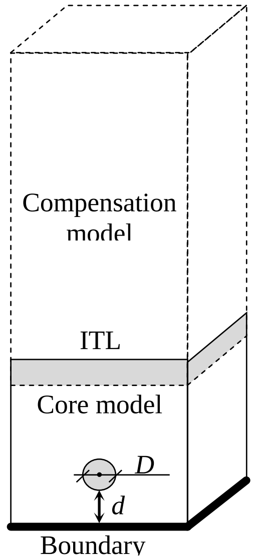

(a) Geometrical configuration of concrete analysis space and rebar

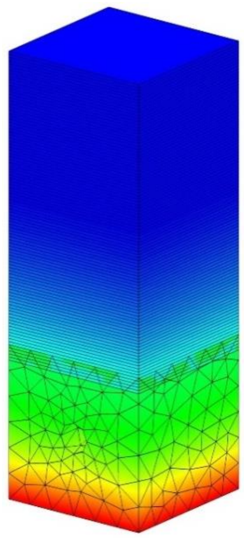

(b) Typical distribution of aggregate and chloride content in concrete

Fig. 20 Geometrical configuration and chloride content distribution of compensation case

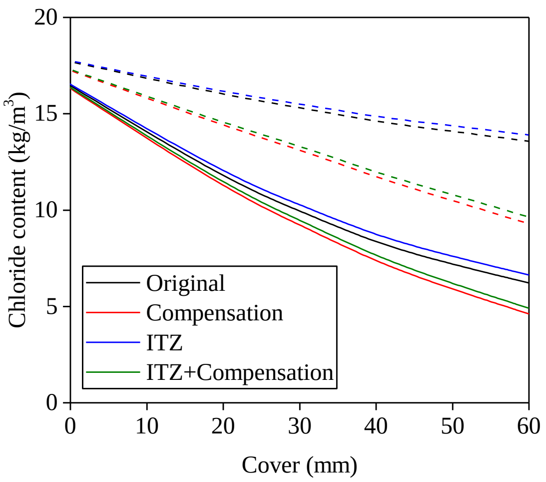

(a) Mean chloride content vs. cover thickness, 16 mm rebar

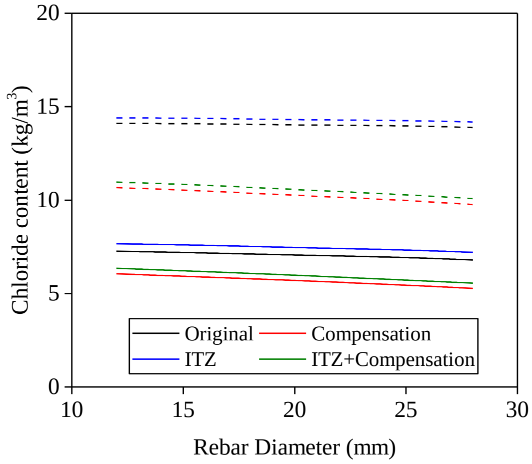

(b) Mean chloride content vs. diameter, 50 mm cover

Fig. 21 Mean chloride content of rebar on center of bottom side (solid-20yr; dashed-50yr)

thickness and 50 mm cover thickness for the comparison of rebar diameters. By means of the random aggregate generation approach and considering reasonable computing loading, three-dimensional samples for each combination of concrete cover thickness and rebar diameter were modeled considering random distribution of aggregate.

Considering three-phase composite of concrete, nodes and elements of ITZ were modeled not only surrounding aggregate, but also on the surface of steel rebar. It also justified to a certain extent that the formation of ITZ on surface of steel rebar in the light of the same mechanism of aggregate. Therefore the same thickness and diffusivity of ITZ on surface of steel were adoted. Chloride content on front of rebar was extracted from the new created nodes on the edge of ITZ elements in terms of the neat surface of steel rebar.

The placement of steel rebar on the center of straight edge was considered. Rebar placed in the center of bottom side of concrete section (Fig. 20(a)) listed in Table 1 were tested. Term *d* denotes the cover thickness and the diameter; *D* of circle refers to diameter of rebar. A three-dimensional mesoscopic core model in the size of 100×100×100 mm was created. In order to guarantee the effect of compensation, 100×100×200 mm total size of compensation model was designed as two times of core model. 10 mm thickness of ITL was considered for compensation process. Apart of ITZ elements surrounding aggregates, new elements adjacent to steel rebar were also modeled by expanding outline. Therefore, chloride content on surface of rebar was extracted from the newly built nodes of ITZ. Both types of cases with compensation and without compensation were studied. Diffusivity of ITZ in D_{ITZ}/D_{CP}=5 was adopted. 50 μm of ITZ thickness was modeled by expanding the edge of aggregate and rebar. Maximum aggregate size in 20mm was considered and Fuller grading was adopted.

Fig. 20(b) showed typical distribution of chloride content within core mesoscopic model and compensated macroscopic model for the cases of rebar placed in center of bottom. The contour clearly described sound transition of chloride content near ITL on both cases and proved the effect of compensation as well.

The curve surface of rebar was meshed into a series of node and nodal chloride content was obtained from result of FE analysis. For all samples of each research case, mean value of chloride content on each nodes around rebar was calculated. Distribution of chloride content developed towards lower-middle, which matched the configuration of boundary condition. Result indicated higher chloride content was obtained for longer period of exposure. Moreover, lower value was observed in the cases with compensation.

Mean chloride content vs. cover thickness for 16 mm rebar and mean chloride content vs. diameter for 50mm cover were summarized in Fig. 21. An obvious result showed lower chloride content in compensation case since solid lines were all under corresponding dashed lines in the figures, which attributed the larger diffusion space in compensation cases.

Another observation was the insignificant difference between the solid line of 'ITZ' and 'ITZ+Compensation' (20 years). Since diffusion of chloride did not exceed the border of core part and compensation part, there was no clearly difference for both diffusion spaces of 'ITZ' and 'ITZ+Compensation', which is the major reason.

The corrosion model regressed by Liu (Liu and Weyers 1998) based on experimental data included the influence of chloride content, temperature, concrete cover resistance and time of cement hydration, which was expressed as

$$\ln(1.08 i_{corr}) = 8.37 + 0.618 \cdot \ln(1.69 Cl) - 3034/T - 0.000105 R_c + 2.32 t^{-0.215} \quad (1)$$

Where, i_{corr} is corrosion current intensity (μA/cm^2); Cl is chloride content (kg/m^3), which was obtained from numerical simulation result of chloride diffusion; T is temperature at the depth of steel surface (in degree Kelvin); R_c is the resistance of the cover concrete (ohms); t is corrosion time duration (years). For corrosion calculation in the following discuss, environmental temperature 293K was adopted. A generally adopted value of concrete resistance 1500Ω was adopted. Besides, pitting of rebar was neglected. With the data chloride content obtained by numerical simulation, the real-time corrosion current rate at each time step of numerical simulation was calculated. The corrosion depth on surface of rebar was calculated as (Šavija *et al.* 2013b)

$$D_{t+\Delta t} = D_t - 0.023 \cdot i_{corr} \Delta t \quad (2)$$

Where, D_i is remaining rebar diameter (mm) at t years, here 20 mm adopted; $D_{i+\Delta t}$ is reduced rebar diameter (mm) at $t+\Delta t$ years.

A single mean chloride content for each time step was calculated as the attacking chloride content for rebar and mean corrosion depth of rebar was calculated based on Eq. (1). Fig. 22(a) (cover thickness) and Fig. 22(b) (rebar diameter) showed corrosion process and characteristics of rebar based on obtained distribution of chloride content around rebar. Ordinate in these figures indicated the ratio of diameter of corroded rebar to initial value.

Since chloride ion diffused within larger space, obtained diagrams showed less corrosion of steel rebar in the cases of compensation. Moreover, slightly more difference was observed between the curves of compensation model (solid) and none- compensation model (dashed).

Moreover, it should be noted that increasing concrete cover provided slight effect on protecting steel rebar from corrosion. The higher diffusivity in ITZ adhering on steel

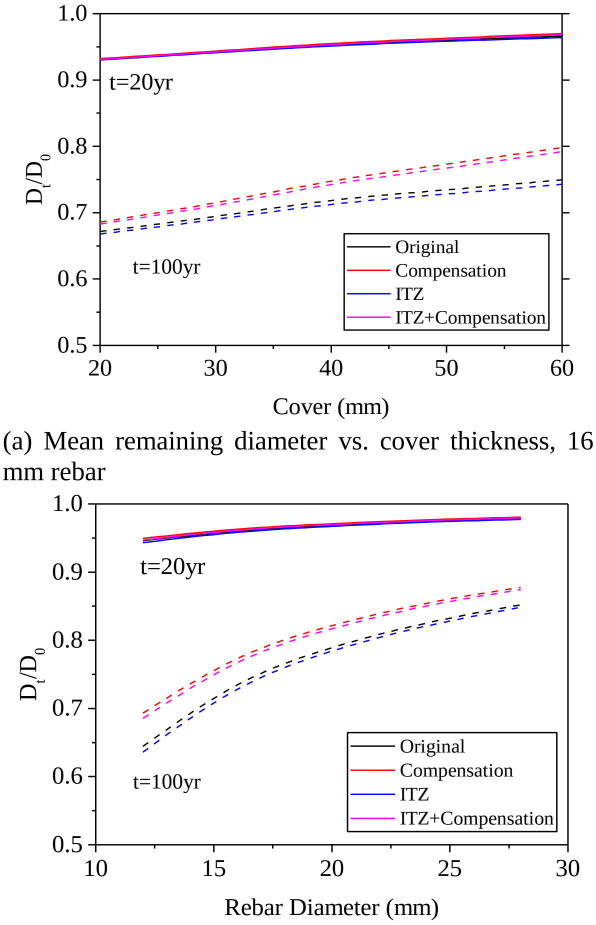

(a) Mean remaining diameter vs. cover thickness, 16 mm rebar

(b) Mean remaining diameter vs. diameter, 50 mm cover

Fig. 22 Mean chloride content of rebar on center of bottom side (solid-20yr; dashed-100yr)

rebar provided an equivalent express channel for diffusion of chloride ion around steel rebar. Thus ITZ actually balanced the difference of depth from surface of concrete for these cases and insignificant difference was observed for cases in different covers. Similar phenomenon was noticed that compensation decreased chloride content on surface of rebar as well as its corrosion degree.

4. Conclusions

This paper presented a study on the approach of three-dimensional multiscale modeling for diffusion of chloride ion within concrete including ITZ. A two-phase integrated model including core part and compensation part was introduced, where both phases were connected by an overlapped zone called Interfacial Transition Layer. Nodes and elements of ITZ in FE model were built by expanding inner surface of aggregates which were randomly generated. Cases considering multiscale and ITZ were studied for obtaining chloride content profile. Moreover, corrosion of rebar on flat surface was discussed by means of the multiscale approach. The conclusions of this study were summarized as follows:

(1) The multiscale approach based on the theory of

compensation for mesoscopic numerical simulation of chloride diffusion within concrete introduced in this paper was applied by means of numerical simulation in three-dimensional space. The presented work showed the influence of compensated model on distribution of chloride content, which enlightened the possible application in future large-scale structural durability analysis for the purpose of optimized size, number of DOFs and time consumption.

(2) Regarding diffusivity and thickness of ITZ, volume fraction and grade of aggregate, effects of ITZ on distribution of chloride were compared in the presented work. Analysis in three-dimensional approach showed significant difference on distribution of chloride content between configuration of ITZ and compensation.

(3) In the light of corrosion model of steel rebar in terms of surrounding chloride content, presence of ITZ and multiscale compensation were discussed by numerical simulation. Result obtained related to the configuration of rebar diameter, concrete cover and exposure period. It was clearly concluded that consideration of both ITZ and compensation changed significantly the distribution of chloride content as well as corrosion process of steel rebar.

Acknowledgements

This paper was sponsored by National Key Research and Development Program of China (2016YFC0701202), project supported by the National Natural Science Foundation of China (51508053) and project support by the Fundamental Research Funds for the Central Universities (106112014CDJZR200016), which were greatly appreciated by the authors.

Reference

Andrade, C., Alonso, C. and Molina, F.J. (1993), “Cover cracking as a function of bar corrosion: Part I-Experimental test”, *Mater. Struct.*, **26**(8), 453-464.

Angst, U., Elsener, B., Larsen, C.K. and Vennesland, Ø. (2009), “Critical chloride content in reinforced concrete-A review”, *Cement Concrete Res.*, **39**(12), 1122-1138.

Bailakanavar, M., Liu, Y., Fish, J. and Zheng, Y. (2012), “Automated modeling of random inclusion composites”, *Eng. Comput.*, **30**(4), 609-625.

Bernard, F. and Kamali-Bernard, S. (2015), “Numerical study of ITZ contribution on mechanical behavior and diffusivity of mortars”, *Comput. Mater. Sci.*, **102**, 250-257.

Biondini, F., Bontempi, F., Frangopol, D.M. and Malerba, P.G. (2004), “Cellular automata approach to durability analysis of concrete structures in aggressive environments”, *J. Struct. Eng.*, **130**(11), 1724-1737.

Biondini, F., Bontempi, F., Frangopol, D.M. and Malerba, P.G. (2006), “Probabilistic service life assessment and maintenance planning of concrete structures”, *J. Struct. Eng.*, ASCE, **132**(5), 810-825.

Caballero, A., López, C.M. and Carol, I. (2006), “3D meso-structural analysis of concrete specimens under uniaxial tension”, *Comput. Meth. Appl. Mech. Eng.*, **195**(52), 7182-7195.

Chen, L., Qian, Z. and Wang, J. (2016), “Multiscale numerical modeling of steel bridge deck pavements considering vehicle-pavement interaction”, *Int. J. Geomech.*, **16**(1), B4015002..

Dridi, W. (2013), “Analysis of effective diffusivity of cement based materials by multi-scale modelling”, *Mater Struct*, **46**(1-2), 313-326.

Du, X., Jin, L. and Ma, G. (2014), “A meso-scale numerical method for the simulation of chloride diffusivity in concrete”, *Finite Elem. Anal. Des.*, **85**, 87-100.

François, R. and Arliguie, G. (1999), “Effect of microcracking and cracking on the development of corrosion in reinforced concrete members”, *Mag. Concrete Res.*, **51**(2), 143-150.

Hiratsuka, Y. and Maekawa, K. (2015), “Multi-Scale and multi-chemo-physics analysis applied to fatigue life assessment of strengthened bridge decks”, *Comput. Plast. XIII: Fund. Appl.*, 596-607.

Li, C.Q. (2000), “Corrosion initiation of reinforcing steel in concrete under natural salt spray and service loading-results and analysis”, *Mater. J.*, **97**(6), 690-697.

Liu, T. and Weyers, R.W. (1998), “Modeling the dynamic corrosion process in chloride contaminated concrete structures”, *Cement Concrete Res.*, **28**(3), 365-379.

Ma, H., Xu, W. and Li, Y. (2016), “Random aggregate model for mesoscopic structures and mechanical analysis of fully-graded concrete”, *Comput. Struct.*, **177**, 103-113.

Maekawa, K., Ishida, T. and Kishi, T. (2003), “Multi-scale modeling of concrete performance integrated material and structural mechanics”, *J. Adv. Concrete Technol.*, **1**(2), 91-126.

Mori, D., Yamada, K., Hosokawa, Y. and Yamamoto, M. (2006), “Applications of electron probe microanalyzer for measurement of Cl concentration profile in concrete”, *J. Adv. Concrete Technol.*, **4**(3), 369-383.

Pan, Z., Chen, A. and Ruan, X. (2015), “Spatial variability of chloride and its influence on thickness of concrete cover: A two-dimensional mesoscopic numerical research”, *Eng. Struct.*, **95**, 154-169.

Pritpal, S.M. and Mahmoud, S.E. (1999), “Flexural strength of concrete beams with corroding reinforcement”, *Struct. J.*, **96**(1), 149-158.

Šavija, B., Luković, M., Pacheco, J. and Schlangen, E. (2013), “Cracking of the concrete cover due to reinforcement corrosion: A two-dimensional lattice model study”, *Constr. Build. Mater.*, **44**, 626-638.

Šavija, B., Pacheco, J. and Schlangen, E. (2013), “Lattice modeling of chloride diffusion in sound and cracked concrete”, *Cement Concrete Compos.*, **42**, 30-40.

Sun, G., Zhang, Y., Sun, W., Liu, Z. and Wang, C. (2011), “Multi-scale prediction of the effective chloride diffusion coefficient of concrete”, *Constr. Build. Mater.*, **25**(10), 3820-3831.

Torres-Acosta, A.A., Navarro-Gutierrez, S. and Terán-Guillén, J. (2007), “Residual flexure capacity of corroded reinforced concrete beams”, *Eng. Struct.*, **29**(6), 1145-1152.

Torres-Acosta Andrés, A. and Martı´nez-Madrid, M. (2003), “Residual life of corroding reinforced concrete structures in marine environment”, *J. Mater. Civil Eng.*, **15**(4), 344-353.

Tu, X., Li, Z., Chen, A. and Pan, Z. (2018), “A multiscale numerical simulation approach for chloride diffusion and rebar corrosion with compensation model”, *Comput. Concrete*, **21**(4), 471-484.

Unger, J.F. and Eckardt, S. (2011), “Multiscale modeling of concrete”, *Arch. Comput. Meth. Eng.*, **18**(3), 341.

Vidal, T., Castel, A. and François, R. (2004), “Analyzing crack width to predict corrosion in reinforced concrete”, *Cement Concrete Res.*, **34**(1), 165-174.

Vidal, T., Castel, A. and François, R. (2007), “Corrosion process and structural performance of a 17 year old reinforced concrete beam stored in chloride environment”, *Cement Concrete Res.*,

37(11), 1551-1561.
Wang, X., Zhang, M. and Jivkov, A.P. (2016), "Computational technology for analysis of 3D meso-structure effects on damage and failure of concrete", *Int. J. Solid. Struct.*, **80**, 310-333.
Wang, Z.M., Kwan, A.K.H. and Chan, H.C. (1999), "Mesoscopic study of concrete I: generation of random aggregate structure and finite element mesh", *Comput. Struct.*, **70**(5), 533-544.
Wu, K., Xu, L., Schutter, G.D., Shi, H. and Ye, G. (2015), "Influence of the interfacial transition zone and interconnection on chloride migration of portland cement mortar", *J. Adv. Concrete Technol.*, **13**(3), 169-177.
Xu, J. and Li, F. (2017), "A meso-scale model for analyzing the chloride diffusion of concrete subjected to external stress", *Constr. Build. Mater.*, **130**, 11-21.
Ren, J.Y.W. (2006), "Generation of spatial convex polyhedron random aggregate model", *ICOME 2006*, Hefei, China.
Zhang, R., Castel, A. and François, R. (2009), "The corrosion pattern of reinforcement and its influence on serviceability of reinforced concrete members in chloride environment", *Cement Concrete Res.*, **39**(11), 1077-1086.
Zhang, R., Castel, A. and François, R. (2010), "Concrete cover cracking with reinforcement corrosion of RC beam during chloride-induced corrosion process", *Cement Concrete Res.*, **40**(3), 415-425.
Zhang, Z. and Zhang, Q. (2017), "Self-healing ability of Engineered Cementitious Composites (ECC) under different exposure environments", *Constr. Build. Mater.*, **156**, 142-151.
Zhang, Z. and Zhang, Q. (2018), "Matrix tailoring of Engineered Cementitious Composites (ECC) with non-oil-coated, low tensile strength PVA fiber", *Constr. Build. Mater.*, **161**, 420-431.
Zhao, Y., Gao, X., Xu, C. and Jin, W. (2009), "Concrete surface chloride ion concentration varying with seasons in marine environment (Chinese)", *J. Zhejiang Univ. (Eng. Sci.)*, **43**(11), 2120-2124.
Zheng, J.J., Wong, H.S. and Buenfeld, N.R. (2009), "Assessing the influence of ITZ on the steady-state chloride diffusivity of concrete using a numerical model", *Cement Concrete Res.*, **39**(9), 805-813.
Zheng, J.J. and Zhou, X.Z. (2013), "Effective medium method for predicting the chloride diffusivity in concrete with ITZ percolation effect", *Constr. Build. Mater.*, **47**, 1093-1098.
Zhu, W., François, R., Fang, Q. and Zhang, D. (2016), "Influence of long-term chloride diffusion in concrete and the resulting corrosion of reinforcement on the serviceability of RC beams", *Cement Concrete Compos.*, **71**, 144-152.
Zhu, Z., Chen, H., Liu, L. and Li, X. (2017), "Multi-scale modelling for diffusivity based on practical estimation of interfacial properties in cementitious materials", *Powder Technol.*, **307**, 109-118.

CC